Ion-Pair Dissociation Dynamics of HCl: Fast Predissociation

Di Song,[†] Kai Liu,[†] Fan-ao Kong,[†,*] Juan Li,[‡] and Yuxiang Mo[‡,*]

The State Key Laboratory of Molecular Reaction Dynamics, Institute of Chemistry, Chinese Academy of Science, Beijing 100190, People's Republic of China, and, Department of Physics and Key Laboratory for Atomic and Molecular Nanosciences, Tsinghua University, Beijing, 100084, People's Republic of China

Received: January 14, 2009; Revised Manuscript Received: March 8, 2009

We have studied the ion-pair dissociation dynamics of $HCl \rightarrow Cl^- (^1S_0) + H^+$ in the 14.41−14.60 eV using tunable XUV laser and the velocity map imaging method. The measured ion-pair yield spectrum has *P*- and *R*-branch resolved vibrational structure, which indicates a predissociation mechanism for the ion-pair dissociation. All of the anisotropy parameters for the angular distribution of the fragments have the limiting values of $\beta = 2$, which suggests that the predissociation occurs via $^1\Sigma^+$ Rydberg states, and is fast in comparison with the rotational period of HCl. To understand the predissociation dynamics, the diabatic potential energy curve of the ion-pair state has been calculated at the MRCI/CAS/vtz level. The experimental and theoretical results obtained in this work have provided a solid foundation for the previously proposed mechanism that the ion-pair dissociation occurs via predissociation of Rydberg states converging to $HCl^+ (A^2\Sigma^+)$.

I. Introduction

The photoionization and photodissociation dynamics of HCl plays important role in understanding the properties of diatomic molecules.[1−7] The ion-pair dissociation of HCl has attracted a great deal of attention because it provides a window to study superexcited states that have excitation energies higher than their first ionization potential energy.[8−11]

By using synchrotron radiation, Yencha et al. measured the Cl^- ion-pair yield spectrum in the energy range 14.4−16.5 eV,[8]

$$HCl + 14.418\ eV \rightarrow H^+ + Cl^-(^1S_0) \qquad (1)$$

They observed a series of resonance structures assigned from the predissociation of Rydberg series, $[A^2\Sigma^+]nl\sigma$, $l = s$, p, and d with $^1\Sigma^+$ symmetry, where $[A^2\Sigma^+]$ represents the state for the ion-core HCl^+. Recently, Hu et al. reported a higher resolution H^+ ion-pair yield spectrum using XUV laser in the 14.4−14.55 eV.[9] The main characteristics of the spectrum obtained by Hu et al. are similar to that reported by Yencha et al.; however, it was found that some detailed structure may need other assignments, such as $[A^2\Sigma^+]nf\sigma$ and $[A^2\Sigma^+]np\pi$.

If the interaction between the Rydberg states and ion-pair state is due to homogeneous coupling, or $\Delta\Omega = 0$, where Ω is the projection of total electronic angular momentum on the molecular axis, then only Rydberg states of $^1\Sigma^+$ symmetry should be excited since the potential energy curve corresponding to eq 1 has $^1\Sigma^+$ symmetry. Although it is reasonable to assume it to be true, there is as yet no concrete experimental evidence to support it. The recent studies on the ion-pair dissociation of Cl_2 showed that the coupling between Rydberg states and ion-pair states usually prefers homogeneous perturbation, however, heterogeneous ($\Delta\Omega = \pm 1$) perturbation does occur.[12,13] It is therefore interesting to study the symmetry properties of Rydberg states excited in the ion-pair dissociation of HCl.

In this work, we report our studies of ion-pair dissociation of HCl in the energy range of 14.41−14.60 eV by using the velocity map imaging method and tunable XUV light produced by nonlinear four-wave mixing. An H^+ ion-pair yield spectrum with resolution higher than that previously reported was obtained. The angular distributions of the photofragments suggest that the predisssociation is a fast process and that all excited Rydberg states have $^1\Sigma^+$ symmetry.

II. Experimental Section

The experimental machine used in this study has previously been described in detail,[12−15] therefore, only a brief summary is given here. The coherent XUV radiation was generated using the resonance enhanced four-wave sum mixing ($2\omega_1 + \omega_2$) in a pulsed Kr jet. An Nd:YAG (YAG-yttrium aluminum garnet) (20 Hz) pumped two dye laser system was used in the experiments. One laser beam (ω_1) was prepared by tripling of a dye laser. The $2\omega_1$ (98 855.1 cm^{-1}) was fixed at the transition of $4p^5(^2P_{1/2})5p[1/2]_0 \leftarrow (4p^6)\ ^1S_0$. The other dye laser was tuned from 530−575 nm. The uncertainties of the XUV photon energies are ± 1 cm^{-1}, and the resolution of the XUV laser was around 0.1 cm^{-1}. For ion-pair yield measurement, the H^+ signals from the ion-pair dissociation were recorded under field-free conditions, and an extraction field of about 600 V/cm was applied after a delay of 400 ns relative to the XUV laser pulse. The XUV light intensity was also recorded for each laser pulse, and the ion-pair yield spectrum has been normalized by the XUV light intensity pulse by pulse. The velocity map imaging technique follows that of Parker and co-workers.[16]

The HCl gas sample was premixed with Ne (Ne 97%, HCl 3%), and the stagnation pressure used was about 1000 Torr at room temperature. In the experiments, the pressures for the molecular beam source and ionization chamber were around 1×10^{-5} and 1×10^{-7} Torr, respectively.

III. Results and Discussion

A. Ion-Pair Yield Spectrum and Its Assignment. Figure 1 shows the H^+ ion yield spectrum from the ion-pair dissociation of HCl in the energy range of 116 276−117 756 cm^{-1}. The spectrum has clearly resolved structure. The ion-pair yield spectrum is assigned to the excitation from $HCl(X^1\Sigma^+)$ to

* To whom correspondence should be addressed. E-mail: kong@iccas.ac.cn; ymo@mail.tsinghua.edu.cn.
† Institue of Chemistry.
‡ Tsinghua University.

10.1021/jp900383z CCC: $40.75
Published on Web 04/08/2009

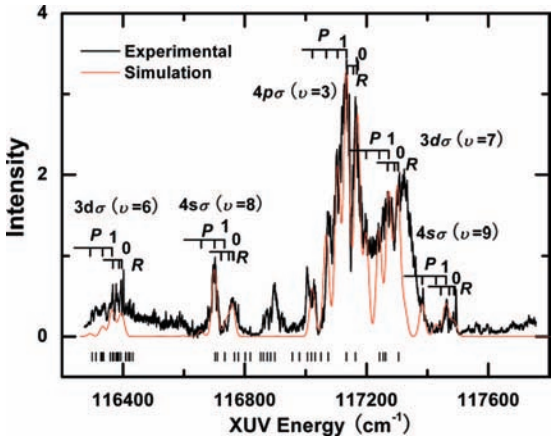

Figure 1. H^+ ion-pair yield spectrum for the ion-pair dissociation of HCl under field free condition. The black curve is the experimental data, and the red curve is the simulation. The Rydberg state assignments including the *P*- and *R*-branches are also shown. There are 44 vertical bars at the bottom representing the energy positions at which the velocity mapping images of H^+ have been recorded. To record the ion-pair yield spectrum, an extraction field of ~600 V/cm was exerted after a delayed of ~400 ns relative to the XUV laser pulses. The H^+ signal intensities have been normalized by the XUV light intensities.

Rydberg series with $^1\Sigma^+$ symmetry, the same as that assigned by Yencha et al. and Hu et al.[8,9] Our imaging experiment (see next section) provides clear evidence of such $^1\Sigma^+ - ^1\Sigma^+$ transitions. The superexcited states further undergo dissociation, leading to the final products H^+ and Cl^- ion-pair.

The spectrum shown in Figure 1 has higher resolution than that previously reported, since a supersonic cooled molecular beam and a high resolution XUV laser was used in the experiments. An apparent characteristic of the spectrum is that there are some sharp dips in the resolved structures, which have not been previously found. The dips arise from the lack of *Q*-branches in the $^1\Sigma^+ - ^1\Sigma^+$ transitions. They hint at the origins of the vibrational bands. The spectrum is not yet rotationally fully resolved. This fact suggests that the predissociation lifetime is short in comparison with the rotational period of HCl.

The energy levels (υ_0) for Rydberg states converging to HCl^+ ($A^2\Sigma^+$, υ^+) are described by the well-known formula,

$$\upsilon_0 = \mathrm{IE}(\upsilon^+) - \frac{R}{(n-\delta)^2} \qquad (2)$$

where $\mathrm{IE}(\upsilon^+)$ is the ionization energy for the transition HCl^+ ($A^2\Sigma^+$, υ^+) ← $HCl(X^1\Sigma^+)$[17], n is the principal quantum number, δ is the quantum defect, and R is Rydberg constant for HCl.

In this energy region, the principal quantum numbers n are very small, 3 or 4; therefore, the electronic structure of the Rydberg states can be taken as Hund's case (a). The line position (υ) for the transition between the Rydberg state $HCl(R^1\Sigma^+, J', \upsilon')$ and the ground-state $HCl(X^1\Sigma^+, J'', \upsilon'' = 0)$ is described by the following:

$$\upsilon = \upsilon_0 + (B'_\upsilon + B''_\upsilon)m + (B'_\upsilon - B''_\upsilon)m^2 \qquad (3)$$

where B'_υ and B''_υ are the rotational constants for Rydberg state and ground state, respectively. $m = -J''$ refers to *P*-branch transition, and $m = J'' + 1$ refers to *R*-branch transition.

Since only a few Rydberg states have been observed in our spectrum, our assignment of Rydberg states simply follows previous studies.[8,9] To determine the vibrational band origins accurately, simulations considering the transition line intensities and coupling strengths between Rydberg states and ion-pair states are necessary, which are difficult tasks at present. We have thus performed empirical simulations for the ion-pair yield spectrum. The rotational constants for Rydberg states were assumed to be the same as those of HCl^+ ($A^2\Sigma^+$) or $B'_\upsilon = 7.505 - 0.331(\upsilon' + 1/2)$.[18,19] The rotational temperature was taken as 60 K, the rotational line intensities for each transition were adjusted to reproduce the shape of the spectrum as closely as possible. The rotational line profiles were assumed as Gaussian functions with a line width of ~21 cm^{-1}.

It can be seen in Figure 1 that the major parts of the spectrum can be explained by the simulation. The unexplained parts may be due to Rydberg series that have not been considered in this work, for example, the Rydberg series of $^1\Sigma^+$ symmetry converging to HCl^+ ($X^2\Pi_g$). The bands in the spectrum are assigned as $[A^2\Sigma^+]4s\sigma(\upsilon = 8,9)$, $[A^2\Sigma^+]4p\sigma(\upsilon = 3)$ and $[A^2\Sigma^+]3d\sigma(\upsilon = 6,7)$, respectively. It is noted that the quantum defect for $3d\sigma$, ~0.81, is smaller than that used previously, ~0.83,[8,9] however, which is closer to the ab initio theoretical value of 0.78.[3] The band origins and quantum defects δ obtained in this analysis are listed in Table 1 along with the previously published data. Since the *P*- and *R*-branches in the ion-pair yield spectrum have been clearly resolved, the vibrational band origins determined in this work are thus more accurate than those reported previously.[8,9]

From the simulation, it is known that the linewidths for Rydberg states are ~21 cm^{-1}, the lifetime of Rydberg states is hence approximated to be $\sim 2.5 \times 10^{-13}$ s that is much smaller than the classical rotational period of HCl $\sim 2 \times 10^{-12}$ s, for a typical rotational constant $B'_{\upsilon=3} = 6.3$ cm^{-1} and $J' = 1$. It is thus expected that the predissociation is a fast process in comparison with the rotational period of molecular rotation, which is further proved by the measurement of angular distribution of H^+ fragments, as discussed below.

B. Angular Distribution of Photofragements. We have recorded the velocity mapping images of H^+ at 44 different excitation energies indicated as vertical bars in Figure 1. Six of the example images are shown in Figure 2. The images were recorded under the electric field strengths of ~700 V/cm, however, it is expected that this would not change the dynamics of ion-pair dissociation very much for photon excitation energies of about ~100 cm^{-1} above the threshold of ion-pair dissociation (116 287 cm^{-1}).[9,12−14]

The H^+ angular distributions can be obtained by extracting the information in the 2D images derived from the Abel transform of the experimental images. The anisotropy parameters β are obtained by fitting the experimental data using the following formula:[21,22]

$$f(\theta) \propto 1 + \beta P_2(\cos\theta) \qquad (4)$$

where θ is the angle between the recoil velocity and the polarization direction of the XUV laser, and $P_2(x)$ is the second order Legendre polynomial. Figure 3 shows the angular distributions extracted from the six images shown in Figure 2, and the fitting curves using eq 4.

It is surprising that all of the measured β values have the limiting values of +2. The results mean that the optical transitions to Rydberg states should be the so-called parallel transitions and the excited Rydberg states have $^1\Sigma^+$ symmetry. Since the ion-pair state also has $^1\Sigma^+$ symmetry, the coupling between the Rydberg state and ion-pair state should occur via homogeneous interaction. However, it is not straightforward to anticipate all of the predissociations coming from the homogeneous perturbation since heterogeneous perturbation ($\Delta\Omega = \pm 1$) may occur due to the coupling between the nuclear rotation and electronic orbital angular momentum.[20] However,

TABLE 1: Band Origins, Assignments and Quantum Defects for Rydberg states in the Ion-Pair Yield Spectrum[a]

	this work		ref 9		ref 8	
assignment	υ_0(cm^{-1})	δ	υ_0 (cm^{-1})	δ	υ_0 (cm^{-1})	δ
3dσ(υ = 6)	116 385	0.810				
4sσ(υ = 8)	116 754	1.888	116 330	1.8978	116 500	1.90
4pσ(υ = 3)	117 155	1.559	117 100	1.5602		1.55
3dσ(υ = 7)	117 294	0.818	116 680	0.8400		0.83
4sσ(υ = 9)	117 482	1.899	117 220	1.8962	117 250	1.90

[a] The vibrational energy levels for HCl^+ ($A^2\Sigma^+$) in our quantum defect calculations are from ref 17, whereas those used in refs 9 and 8 are different from ours.

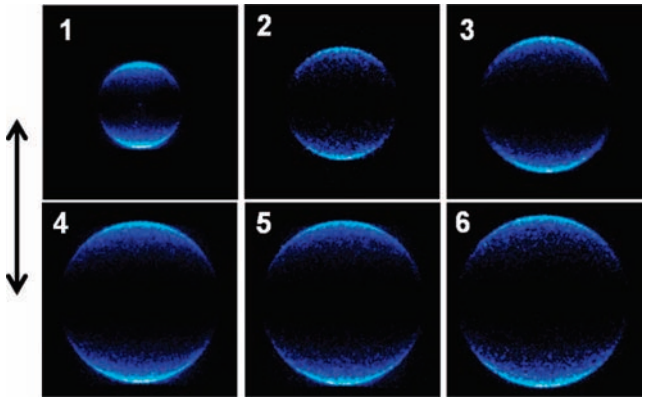

Figure 2. Experimental raw images of H^+ fragments from the ion-pair dissociation of HCl under electric field of ~700V/cm. The polarization of the XUV laser is indicated. The excitation energies are 116 358, 116 702, 116 899, 117 134, 117 164, 117 262 cm^{-1} for images 1 to 6, respectively.

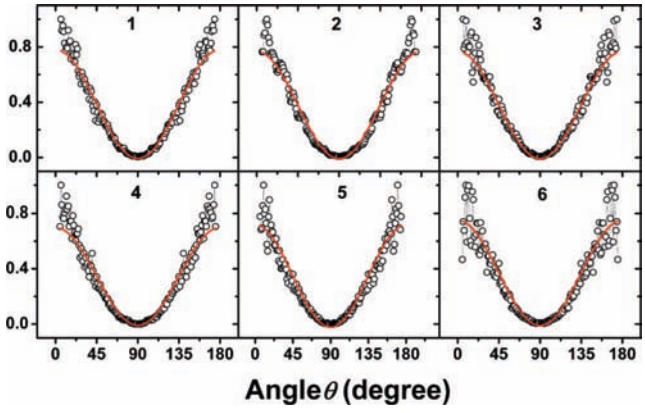

Figure 3. Angular distributions of H^+ fragments obtained from the inverse Abel transforms of the corresponding images showing in Figure 2. The small circles represent the experimental data, and the solid lines are the least-squares fittings using eq 4. The noises near 0° and 180° are from Abel transforms, which have not been included in the fittings. The β values equal 2 for all the fitting curves.

even for parallel transitions, the anisotropy parameters β for the angular distribution of the photofragments may be smaller than the limiting value +2 due to the finite lifetime of the predissociated Rydberg states. Our results provide concrete experimental evidence showing that the predissociation occurs via Rydberg states of $^1\Sigma^+$ symmetry, and is fast in comparison with the rotational period of HCl, which is also supported by the ion-pair yield spectrum.

C. The Potential Energy Curve (PEC) and the Ion-Pair Dissociation Mechanism. The ion-pair state of H^+-Cl^- is usually designated as $V^1\Sigma^+$, which is the second $^1\Sigma^+$ state of HCl. The PEC for $V^1\Sigma^+$ has been calculated in 1982 and also described later by different models.[8,10,11,23,24] In the energy region we are interested in, the calculation is very difficult because

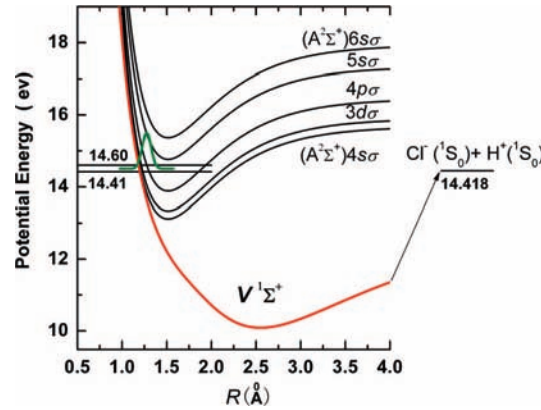

Figure 4. Diabatic PEC for HCl ion-pair state calculated at the level of MRCI/CASSCF/vtz. The diabatic means that the electronic configurations involving the Rydberg electron have not been included in the calculation. The PECs for Rydberg states are by shifting that of HCl^+ ($A\ ^2\Sigma^+$) to the experimentally determined energy position. The PEC of HCl^+ ($A\ ^2\Sigma^+$) is described by a Morse potential with parameters from ref 17. The nuclear wave function for HCl ($X^1\Sigma^+$, υ = 0) is also shown in the figure to display the Franck−Condon region.

there is strong interaction between the ion-pair state and various $^1\Sigma^+$ Rydberg states converging to HCl^+ ($A^2\Sigma^+$). We thus calculated the diabatic PEC for the ion-pair state in which the Rydberg states were not taken into the consideration. The calculation was performed at the level of multireference internally contracted configuration interaction (MRCI) using the MOLPRO software package.[25] The reference functions for MRCI were from the complete active space-SCF (CASSCF) calculation employing the VTZ basis sets. In the calculation, the active orbital space was $(4\sigma)(5\sigma)(2\pi)(6\sigma)$, and the core orbitals were $(1\sigma)^2(2\sigma)^2(3\sigma)^2(1\pi)^4$.

Since the precise PECs for Rydberg states are also difficult to calculate, we assumed that the PECs for Rydberg states have the same shape as that of HCl^+ ($A^2\Sigma^+$). The PECs are described by Morse potential. The parameters in the Morse function are adapted from ref 17. The relative energies of the Rydberg states are from our spectral data.

Figure 4 shows the calculated PECs for the diabatic ion-pair state and the Rydberg states. The vibrational wave function of the ground-state HCl($X^1\Sigma^+$,υ = 0) is also displayed to show the Franck−Condon region. It can be seen from Figure 4 that in the energy region of 14.4−14.6 eV the ion-pair potential is out of the Franck−Condon region. Therefore, the direct excitation from the ground-state to the ion-pair state is difficult. However, an optical excitation to the Rydberg states following a transition to the ion-pair state would be very possible.

The rate of predissociation depends on the coupling strength between the ion-pair state and the Rydberg state. The coupling strength is a product of two matrix elements: electronic coupling and vibrational coupling.[20] At short bond distance, R, both

factors are favorable for the interaction between ion-pair state and the Rydberg state. The reasons are as follows:

(a) A tight coupling between the nuclear wave function of the ion-pair state and that of the Rydberg state could occur at small R, as can be seen from Figure 4.

(b) The electronic configuration for the ion-pair state consists mainly two configurations: $(4\sigma)^2(5\sigma)^1(2\pi)^4(6\sigma)^1$ and $(4\sigma)^2$-$(5\sigma)^2(2\pi)^4$. For short bond distances (R smaller than 2.1 Å), the calculations at the level of MRCI/CASSCF/vtz show that the main electronic configuration is $(4\sigma)^2(5\sigma)^1(2\pi)^4(6\sigma)^1$, whereas for long distances (R larger than 2.1 Å), the main electronic configuration is $(4\sigma)^2(5\sigma)^2(2\pi)^4$. The Rydberg states converging to HCl^+ ($A^2\Sigma$) have the electronic configurations of $(4\sigma)^2$-$(5\sigma)^1(2\pi)^4(nl\sigma)$, $l = s$, p, and d, which differ by one orbital to $(4\sigma)^2(5\sigma)^1(2\pi)^4(6\sigma)^1$, the configuration preferred at small R. Hence, the electrostatic interaction between the ion-pair state and the Rydberg state may take place easily at short bond distances.

For the above reasons, it is expected that the predissociation between the ion-pair state $V^1\Sigma^+$ and Rydberg state $(4\sigma)^2$-$(5\sigma)^1(2\pi)^4(nl\sigma)$ could occur as suggested previously.[8] Since the predissociation is fast as shown by our experimental results, the coupling between the ion-pair state $V^1\Sigma^+$ and Rydberg state $(4\sigma)^2(5\sigma)^1(2\pi)^4(nl\sigma)$ is expected to be strong.

IV. Conclusions

The ion-pair dissociation dynamics of HCl has been studied in the 14.41−14.60 eV by measuring the ion-pair yield spectrum and the velocity mapping images of H^+ fragments. The ion-pair yield spectrum has P- and R-branch resolved vibrational structures, which lead to more accurate assignments of band origins for $^1\Sigma^+$ Rydberg states involved in the predissociation processes. The measured angular distributions of the photofragments provide concrete experimental evidence that the ion-pair dissociations are from parallel transitions and the predissociations are fast in comparison with the rotational period of HCl, which is also supported by the linewidths of the Rydberg states in the ion-pair yield spectrum. The diabatic PEC of the ion-pair state has been calculated at the MRCI/CAS/vtz level. Combining the experimental and theoretical results, it is concluded that the ion-pair dissociation occurs via the predissociation of $^1\Sigma^+$ Rydberg states converging to HCl^+ ($A^2\Sigma^+$), which supports the previously proposed predissociation mechanism.[8]

Acknowledgment. This work is funded by Projects 20673066, 20773076, and 10734040 supported by the National Science Foundation of China, and Project 2007CB815200 supported by NKBRSF of the China.

References and Notes

(1) Natalis, P.; Pennetreau, P.; Longton, L.; Collin, J. E. *Chem. Phys.* **1982**, *73*, 191.

(2) White, M. G.; Leroi, G. E.; Ho, M.-H.; Poliakoff, E. D. *J. Chem. Phys.* **1987**, *87*, 6553.

(3) Lefebvre-Brion, H.; Dehmer, P. M.; Chupka, W. A. *J. Chem. Phys.* **1988**, *88*, 811.

(4) Frohlich, H.; Guyon, P. M.; Glass-Maujean, M. *J. Chem. Phys.* **1991**, *94*, 1102.

(5) Liyanage, R.; Gordon, R. J.; Field, R. W. *J. Chem. Phys.* **1998**, *109*, 8374.

(6) Yencha, A. J.; Cormack, A. J.; Donovan, R. J.; Hopkirk, A.; King, G. C. *Chem. Phys.* **1998**, *238*, 109.

(7) Chichinin, A. I.; Maul, C.; Gericke, K. H. *J. Chem. Phys.* **2006**, *124*, 224324.

(8) Yencha, A. J.; Kaur, D.; Donovan, R. J.; Kvaran, A.; Hopkirk, A.; Lefebvre-Brion, H.; Keller, F. *J. Chem. Phys.* **1993**, *99*, 4986.

(9) Hu, Q. J.; Melville, T. C.; Hepburn, J. W. *J. Chem. Phys.* **2003**, *119*, 8938.

(10) Romanescu, C.; Manzhos, S.; Boldovsky, D.; Clarke, J.; Loock, H.-P. *J. Chem. Phys.* **2004**, *120*, 767.

(11) Romanescu, C.; Loock, H.-P. *J. Chem. Phys.* **2007**, *127*, 124304.

(12) Zhou, C.; Hao, Y.; Mo, Y. *J. Phys. Chem. A* **2008**, *112*, 8263.

(13) Hao, Y.; Zhou, C.; Mo, Y. *J. Phys. Chem. A*, **2009**, *113*, 2294.

(14) Hao, Y.; Zhou, C.; Mo, Y. *J. Phys. Chem. A*. **2005**, *109*, 5832.

(15) (a) Yang, J.; Hao, Y.; Li, J.; Zhou, C.; Mo, Y. *J. Chem. Phys.* **2005**, *122*, 134308. (b) Yang, J.; Hao, Y.; Li, J.; Zhou, C.; Mo, Y. *J. Chem. Phys.* **2007**, *127*, 209901.

(16) Eppink, A. T. J. B.; Parker, D. H. *Rev. Sci. Instrum.* **1997**, *68*, 3477.

(17) Edvardsson, D.; Baltzer, P.; Karlsson, L.; Lundqvist, M.; Wannberg, B. *J. Electron Spectrosc. Relat. Phenom.* **1995**, *73*, 105.

(18) Saenger, K. L.; Zare, R. N.; Mathews, C. W. *J. Mol. Spectrosc.* **1976**, *61*, 216.

(19) Sheasley, W. D.; Mathews, C. W. *J. Mol. Spectrosc.* **1973**, *3*, 420.

(20) Lefebvre-Brion, H.; Field, R. W. *The Spectra and Dynamics of Diatomic Molecules*; Elsevier Academic Press: Amsterdam, 2004.

(21) Zare, R. N.; Herschbach, R. D. *Proc. IEEE.* **1963**, *51*, 173.

(22) Mo, Y.; Suzuki, T. *J. Chem. Phys.* **1998**, *108*, 6780.

(23) Stevens, W. J.; Krauss, M. *J. Chem. Phys.* **1982**, *77*, 1368.

(24) Bettendorff, M.; Peyerimhoff, S. D.; Buenker, R. *J. Chem. Phys.* **1982**, *66*, 261.

(25) MOLPRO, version 2006.1, a package of ab initio programs, Werner, H. J.; Knowles, P. J.; Lindh, R.; Manby, F. R.; Schutz, M. See http://www.molpro.net.

JP900383Z